
Science
Robotics
SEPTEMBER 2017
AAAS

BIOMIMETICS

# A biorobotic adhesive disc for underwater hitchhiking inspired by the remora suckerfish

Yueping Wang,[1]* Xingbang Yang,[1,2]* Yufeng Chen,[3]* Dylan K. Wainwright,[4] Christopher P. Kenaley,[5] Zheyuan Gong,[1] Zemin Liu,[1] Huan Liu,[6] Juan Guan,[7] Tianmiao Wang,[1] James C. Weaver,[3] Robert J. Wood,[3†] Li Wen[1†]

Copyright © 2017 The Authors, some rights reserved; exclusive licensee American Association for the Advancement of Science. No claim to original U.S. Government Works

**Remoras of the ray-finned fish family Echeneidae have the remarkable ability to attach to diverse marine animals using a highly modified dorsal fin that forms an adhesive disc, which enables hitchhiking on fast-swimming hosts despite high magnitudes of fluid shear. We present the design of a biologically analogous, multimaterial biomimetic remora disc based on detailed morphological and kinematic investigations of the slender sharksucker (*Echeneis naucrates*). We used multimaterial three-dimensional printing techniques to fabricate the main disc structure whose stiffness spans three orders of magnitude. To incorporate structures that mimic the functionality of the remora lamellae, we fabricated carbon fiber spinules (270 μm base diameter) using laser machining techniques and attached them to soft actuator–controlled lamellae. Our biomimetic prototype can attach to different surfaces and generate considerable pull-off force—up to 340 times the weight of the disc prototype. The rigid spinules and soft material overlaying the lamellae engage with the surface when rotated, just like the discs of live remoras. The biomimetic kinematics result in significantly enhanced frictional forces across the disc on substrates of different roughness. Using our prototype, we have designed an underwater robot capable of strong adhesion and hitchhiking on a variety of surfaces (including smooth, rough, and compliant surfaces, as well as shark skin). Our results demonstrate that there is promise for the development of high-performance bioinspired robotic systems that may be used in a number of applications based on an understanding of the adhesive mechanisms used by remoras.**

## INTRODUCTION

Since Aristotle's time, humans have been fascinated by the remarkable structure of the remora's adhesive disc (*1*). The eight species of remoras within the ray-finned fish family Echeneidae have the remarkable ability to "hitchhike," or adhere, to a wide range of biological and nonbiological surfaces, including boat hulls, sharks and rays, teleost fishes, cetaceans, sea turtles, and even human divers (*2*). In the case of dolphins, for example, remoras can remain attached while hosts leap out of water and spin with high rotational speeds (*3*). This hitchhiking behavior affords remoras easier access to food from messy-eating hosts and host parasites and protection from predators (*4*). The greatest advantage of this behavior is the reduced energy expenditure associated with movement: By attaching to swimming hosts, remoras can be transported over large distances with minimal effort (*5*). This hitchhiking behavior and corresponding energy savings are enabled by an adhesive disc on the remora's cranium—a modified dorsal fin that represents one of the most extraordinary adaptations within the vertebrates (Fig. 1A) (*6*, *7*).

Although some mechanisms of adhesion in biological systems have been well documented, the van der Waals forces used by geckos (*8*) or the capillary forces by tree frogs (*9*, *10*), terrestrial gastropods (*11*), and beetles (*12*, *13*) are of limited utility in underwater environments. In contrast to their terrestrial counterparts, adhesion mechanisms in aquatic species, such as in the clingfish's suction disc, often rely on a disc's ability to conform to a surface and create a seal (*14*, *15*). The remora's complex disc system, by comparison, is unique and is composed of integumentary structures and musculoskeletal linkages, including a soft disc lip to maintain a seal in addition to rotating, spinule-covered lamellae in the disc interior to aid in attachment. As a result, the biomechanical basis of this high-performance adhesive behavior has recently attracted growing attention (*3*, *6*, *16*).

In many recent studies, biologically inspired robotic platforms (*17*–*20*), state-of-the-art three-dimensional (3D) printing technologies (*21*–*23*), and soft robotic systems (*24*–*29*) have been developed to investigate biomechanical questions related to the locomotion of jumping, swimming, and crawling. In an expansion of this previous work, we fabricated and tested a biomimetic remora disc. In contrast to previous studies that focused primarily on anatomical descriptions, our current efforts focused on the fabrication of a synthetic composite remora disc and therefore permitted a detailed investigation of remora morphological features (i.e., the soft lamella tissue overlay, rigid spinules, and rotatable motion of the lamellae) and their related effects on underwater adhesion under controlled experimental conditions.

Inspired by morphological and kinematic analyses of the adhesive disc from the slender sharksucker, *Echeneis naucrates*, we created a multimaterial 3D-printed prototype that contains composite lamellae lined with ca. 1000 of at-scale carbon fiber spinules, which were fabricated through laser machining; the lamella pitching motion is controlled by lightweight, compliant, soft pneumatic actuators. A detailed description of our design and fabrication workflow is provided in Materials and Methods. Using our remora disc prototype, we investigated the effect of morphological and kinematic features on the disc's adhesive performance on surfaces of different roughness. On the basis of

[1]School of Mechanical Engineering and Automation, Beihang University, Beijing, China. [2]School of Biological Science and Medical Engineering, Beihang University, Beijing, China. [3]John A. Paulson School of Engineering and Applied Sciences and Wyss Institute for Biologically Inspired Engineering, Harvard University, Cambridge, MA 02138, USA. [4]Museum of Comparative Zoology, Harvard University, Cambridge, MA 02138, USA. [5]Department of Biology, Boston College, Boston, MA 02215, USA. [6]School of Chemical Science and Engineering, Beihang University, Beijing, China. [7]School of Material Science and Engineering, Beihang University, Beijing, China.
*These authors contributed equally to this work.
†Corresponding author. Email: liwen@buaa.edu.cn (L.W.); rjwood@eecs.harvard.edu (R.J.W.)

Downloaded from http://robotics.sciencemag.org/ by guest on September 23, 2017

the experimental results from these studies (such as disc chamber pressure, pull-off force, and frictional force), we further combined the biomimetic adhesive disc prototype with an underwater vehicle to explore remora-like applications of our system by transitioning from swimming to attached states on a variety of surfaces.

## RESULTS

### Morphology of the biological remora disc

Within the remora disc interior (Fig. 1A), consecutive rows of slightly overlapping lamellae are distributed in a bilaterally symmetrical fashion (Fig. 1B). The number of rows of lamellae varies across remora species,

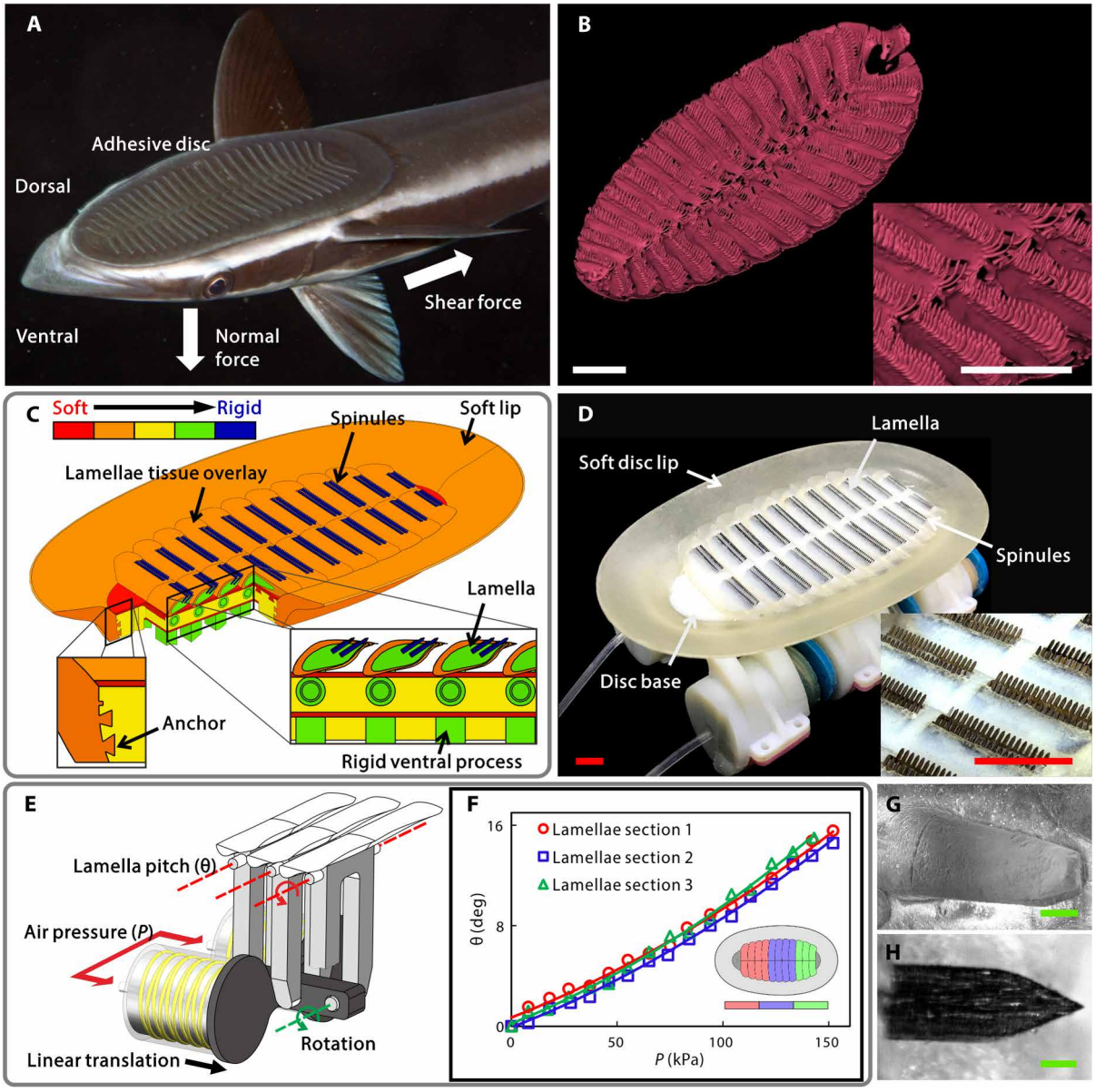


**Fig. 1. Morphology structure of the remora's adhesive disc and our biomimetic prototype design with mechanical elements and mechanisms.** (**A**) Dorsolateral view of the slender sharksucker, *E. naucrates*. The arrows indicate the direction of friction and pull-off force. [Photo credit: Klaus M. Stiefel.] (**B**) 3D reconstructed model of the remora disc based on microCT data (resolution, 35 μm). (Inset) Closer image of the lamellae and rows of spinules. Scale bars, 10 mm. (**C**) CAD model of the biomimetic remora disc. The principal elements of the disc were assigned multiple materials represented by different colors. The spinules have the greatest stiffness (blue), and the materials in the main body include a fully rigid material [e.g., the ventral process and the lamella plate (green)], a medium rigid material [e.g., the disc base (yellow)], and a flexible material [e.g., the disc lip and soft lamella tissue overlay (orange)]. From the cross-sectional view, the edge of the rigid disc base penetrates into the soft lip and forms a cross-connected anchor-like structure (left inset). (Right inset) The biomimetic lamellae are composed of both a rigid skeleton (green) and a soft lamella tissue overlay (orange). For more data about the stiffness of the materials, refer to table S5. (**D**) Photograph of the biomimetic remora adhesive disc prototype (disc pad length, 127 mm; width, 62 mm). Scale bars, 10 mm. (Inset) A higher-magnification view showing the rows of composite lamellae embedded with carbon fiber spinules. (**E**) Drive mechanism for lamella pitch motions, which translates the linear movement of the soft actuators (driven by a pneumatic system) into the rotational movement of the lamellae. Animation of the lamella pitching motion can be seen in movie S3. Lateral view of the actuated disc prototype is provided in movie S4. (**F**) Pitch angle θ of the three sections of the biomimetic disc lamellae (actuated by three pairs of actuators) versus the input air pressure *P*. (**G**) ESEM image of higher-magnification views of a single biological spinule. (**H**) Optical microscopy image of a single carbon fiber spinule fabricated by laser machining. Scale bars, 100 μm (G and H).

Downloaded from http://robotics.sciencemag.org/ by guest on September 23, 2017

with different species having between 10 and 30 rows of lamellae in total (*30*). These lamellae are partially covered by a thin layer of soft tissue that connects laterally with the soft fleshy lip surrounding the disc (*2*, *31*). Through integration with the lamella ventral process, erector and depressor muscles that lie beneath the disc base can rotate the lamellae up or down, in a similar manner by which teleost fish can rotate their spiny dorsal fins to an erect or depressed state (*2*, *32*–*34*). Each lamella row has two to three rows of small rigid spines called spinules (Fig. 1B, inset), and thus, an entire remora disc can contain more than a thousand of these fine structures. The biological spinules have a cone-shaped geometry with an average diameter of 270 μm at their base, a height of approximately 500 μm, and a spacing of 250 μm between adjacent spinules (Fig. 1G). Detailed morphological data on body length, disc dimensions (length, width, and area), mean spanwise length of perpendicular lamellae, lamella spacing, and other disc components are included in table S1.

## Biomimetic remora disc prototype

On the basis of the morphological features of the natural remora disc, we successfully fabricated a biologically inspired, multimaterial structural analog (Fig. 1D). The disc prototype was 127 mm long and 72 mm wide, with a mass of 129 g. The prototype contained a soft lip at the periphery and 11 consecutive rows of overlapped lamellae made of composite materials, each of which contained a linear array of rigid carbon fiber spinules (Fig. 1D). The remora disc prototype was made of a fully rigid material for the skeletal elements (e.g., ventral process and mechanical linkages), a less rigid material for the disc base (e.g., lamella plates and disc base), and a flexible material to allow surface conformation (e.g., disc lip and the soft tissue enveloping the lamella plate) (Fig. 1C). The material stiffness of the 3D-printed disc components spanned three orders of magnitude from flexible to rigid (1.1 to 3000 MPa; table S5). Two rows of laser-cut carbon fiber spinules were installed on the top edge of the lamellae at an angle of 33.7° relative to the horizontal plane, identical to the spinule angle found in *E. naucrates*. Each carbon fiber spinule was 270 μm and terminates in a sharp tip (Fig. 1H).

To mimic the functions of the lamella erector and depressor muscles of the biological remora disc, we used pneumatic, fiber-reinforced soft actuators that connected with the ventral process of the biomimetic lamellae and moved linearly when pressurized pneumatically (Fig. 1E and movie S3). The linear elongation of the soft actuator was converted to the lamella pitching motion through a linkage bar mechanism. The relationship between the lamella pitch angle and the air pressure of the soft actuator was quantified experimentally (Fig. 1F). Upon pressurization, the lamella pitch angle could be precisely controlled between 0° (a biological lamellae's default "down" state) and 16° (a biological lamellae's fully "raised" state) based on the input pneumatic pressure (from 0 to 160 kPa). A comprehensive list of the prototype disc's physical parameters is provided in table S2.

## Biological and biomimetic remora disc kinematics

Observations of the disc functionality revealed that live remoras can actively raise up or fold down rows of lamellae in the center of the adhesive disc, creating a suction seal to the substrate with the soft outer lip. The length, adhesive disc area, and mass of live remoras are in the range of 273 to 324 mm, 11.0 to 19.0 $cm^2$, and 54.9 to 86.9 g, respectively (table S1). We found that remoras fold down their lamellae while sliding along a surface, with the marker point (labeled A in Fig. 2) on the lamellae moving posteriorly up to an amplitude, $\Delta d$ (the displacement of marker points projected on the $x$ axis), of 0.32 mm (Fig. 2). Remoras that intend to stop and adhere to a surface raise up their lamellae, with the marker point moving anteriorly up to an amplitude of 0.25 mm (Fig. 2A). A demonstration of the lamella movement in a live remora is demonstrated in movie S2. We used a nondimensional parameter ($u$; $u = \Delta d/L$, where $L$ represents the distance between two adjacent lamellae) to account for the difference in disc lengths between different remoras and the biomimetic prototype disc to evaluate the lamella pitch motion during attachment. The dimensionless amplitude $u$ of the lamella movement varied significantly for different attachment events (Fig. 2C and fig. S8A). Experimental results show that $u$ ranges from $2.3 \times 10^{-2}$ to $13.7 \times 10^{-2}$ for the folding down of the lamellae and from $2.0 \times 10^{-2}$ to $14.8 \times 10^{-2}$ for the raising up. Statistical analysis showed no significant difference in the dimensionless amplitude ($u$) between raising up and folding down motions of the lamellae [analysis of variance (ANOVA), df = 73, $F = 0.08$, $P = 0.78$] (Fig. 2E).

By pressurizing and depressurizing the three pairs of soft actuators in sequence, the disc prototype can mimic the natural lamella movement (raising and folding) during attachment events. Both tilted 45° top view and side view of the disc prototype are provided in movie S4. Undulation of the lamellae through a differential in actuator timing was developed and is shown in movie S4 for demonstration purposes. For ease of visualization, each of these two motions was performed while the disc prototype was attached to a transparent glass surface underwater (movie S4).

The biomimetic lamellae of our prototype produced pitch motion amplitudes ($u = 0$ to $14.8 \times 10^{-2}$) that covered the range of moving amplitudes of biological lamellae (Fig. 2E). The kinematic profiles of three motion sequences during both raising up (Fig. 2D) and folding down (fig. S8B) lamella movements are quite similar to those found in the biological remora (Fig. 2C and fig. S8A). A comparison of raising and folding motions between the live remora and the biorobotic prototype is available in movie S5.

To further characterize the movement of the biomimetic lamellae, we fabricated a second prototype with a clear disc edge that permitted visualization of the contact between the lamellae and the substrate using a microlens digital camera (section S6). This experimental approach was essential because lateral-view visualization was impossible to achieve in the live remora experiments. Using this second prototype, we were able to visualize the transition of lamellae (with spinules) from a folded ($u = 0$, lamella pitch angle $\theta = 0$) to a raised configuration ($u = 14.8 \times 10^{-2}$, $\theta = 16°$) while in contact with a smooth surface (Fig. 2H). The marker point on the biomimetic lamellae moved anteriorly with an amplitude ($\Delta d$) of 1.04 mm. The soft tissue overlay and rigid spinules made no contact with the smooth surface in the folded-down state ($u = 0$). However, in the raised-up state, the lamella soft tissue overlay and the rigid spinules engaged with the surface. The contact zone between the lamella soft tissue overlay (the translucent component) and the smooth substrate is indicated in Fig. 2H.

The lamella pitch motion induced negative pressure between the disc interior and the ambient environment. By gradually raising up the lamellae, that is, increasing $\theta$ from 0° to 16°, the pressure of the prototype chamber varied from 0 to −3 kPa when the disc was attached to a smooth substrate (fig. S9).

## Force results

The biomimetic remora disc generates considerable pull-off force in the ambient underwater environment (fig. S6), measuring up to 436.6 ± 16.0 N (error values are ±1 SEM) on the smooth surface (Fig. 3A), which was approximately 340 times the weight of the disc prototype (0.129 kg). The pull-off forces ($F_d$) varied with different substrate roughness. The

Downloaded from http://robotics.sciencemag.org/ by guest on September 23, 2017

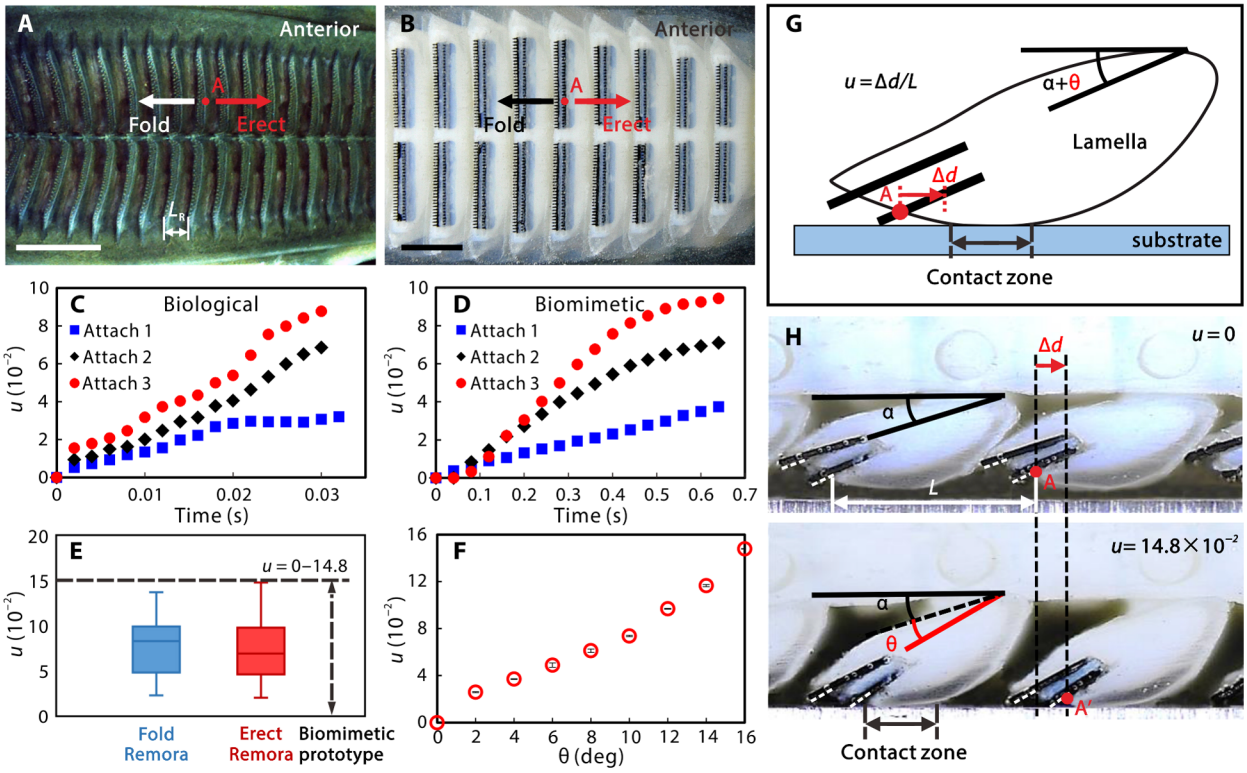


**Fig. 2. Lamella kinematics of the adhesive disc in a live remora and a biorobotic disc prototype.** (**A**) Dorsal view of a live remora's adhesive disc ($L_R$ represents the distance between two adjacent lamellae of the live remora) and (**B**) the biomimetic remora disc prototype attached to a transparent glass substrate. The representative marker point A on the lamella moves anteriorly when the lamellae are raised up and moves posteriorly when the lamellae are folded down. The displacement profiles of the representative marker points for the lamellae of a live remora (**C**) and the biomimetic prototype (**D**) were provided in the raised state ($u = \Delta d/L$, where $L$ represents the distance between two adjacent biomimetic lamellae of the prototype and $\Delta d$ is the displacement of marker point projected in the $x$ axis shown in fig. S1B, which is calculated by instantaneous $x$ value of marker point subtracting the initial $x$ value of marker point). The original point indicates the initial position of the marker point. Profiles for folding down are provided in fig. S8. (**E**) Statistical analysis of lamella kinematics for the remora and biomimetic disc. The lamella rotational range of the biomimetic disc ($u = 0$ to $14.8 \times 10^{-2}$; indicated by black dashed line) is greater than that found in live remoras for both erect and fold motions and can be actively controlled within that range. (**F**) Dimensionless amplitude $u$ of the disc prototype versus lamella pitch angle (θ). (**G**) Schematic view of the lamellae interacting with a substrate. α denotes the angle between the disc lamellae (at the initial fold state) and the horizontal plane, whereas θ denotes the lamella dynamic pitch angle. The contact zone between the lamella soft tissue overlay and the substrate is also illustrated. (**H**) Contact visualization between the biomimetic lamellae and a smooth substrate from side views. Lamellae are composed of both a rigid material (white) and a soft tissue overlay (translucent). Side view of lamellae with the spinules raised from the initial folded state ($u = 0$; top) to the erected state ($u = 14.8 \times 10^{-2}$, θ = 16°; bottom) while in contact with a smooth surface. When the lamellae are raised, the marker point A moved to A′ with a displacement $\Delta d$ (1.04 mm) in the direction of the vector arrows.

disc prototype produced 163.7 ± 3.8 N on real shark skin (from the shortfin mako, *Isurus oxyrinchus*) and 117.8 ± 0.7 N on synthetic rough surfaces (surface roughness $R_a$ = 200 μm). The pull-off stress $\sigma_z$ ($\sigma_z = F_d/A$, where $A$ represents the area of the disc pad) ranged from 15.8 ± 0.1 kPa on rough surfaces to 58.4 ± 2.1 kPa on smooth surfaces. We also observed that the disc volume and the pressure differential between the inside and outside of the disc chamber increased during the pull-off process (fig. S10). The edges of the soft disc lip deformed toward the center of the disc, eventually caving inward and causing the attachment to fail; both pressure and force values dropped to zero once adhesive failure occurred. The disc lamellae also lost contact with the substrate during application of ventrally directed normal forces, suggesting that the normal adhesion force could be primarily attributed to the suction generated by sealing of the soft lip.

We further investigated the effects of both the lamella pitch angle (which correlates with the height change of the lamellae) and the presence of rigid spinules on the adhesive performance of the disc on surfaces of different roughness. In particular, we focused on the role of these structures in the generation of frictional forces during the application on the posteriorly directed forces, a scenario that models fluid drag experienced by a remora when its host is swimming. The instantaneous posterior frictional forces and maximum frictional force of the disc prototype over a range of different lamella pitch angles on the rough surface ($R_a$ = 200 μm) are shown in Fig. 3B. On smooth surfaces ($R_a$ = 0 μm), the average frictional enhancement for all pitch angles (θ) was 8.1 N for the lamellae with spinules and 6.3 N for the lamellae without spinules (Fig. 3C). From the color-shaded area in Fig. 3C, the contribution of the lamella soft tissue overlay to the frictional enhancement is significant, and the spinules do not contribute appreciably to frictional forces on smooth surfaces. Conversely, on the rough surface ($R_a$ = 200 μm), the average frictional enhancement is 1.49 N for the prototype with spinules and 0.17 N in the spinule-free control (Fig. 3D). In contrast, in trials on the real shark skin surface (average roughness $R_a$ = 120 μm), the prototype generated

Downloaded from http://robotics.sciencemag.org/ by guest on September 23, 2017

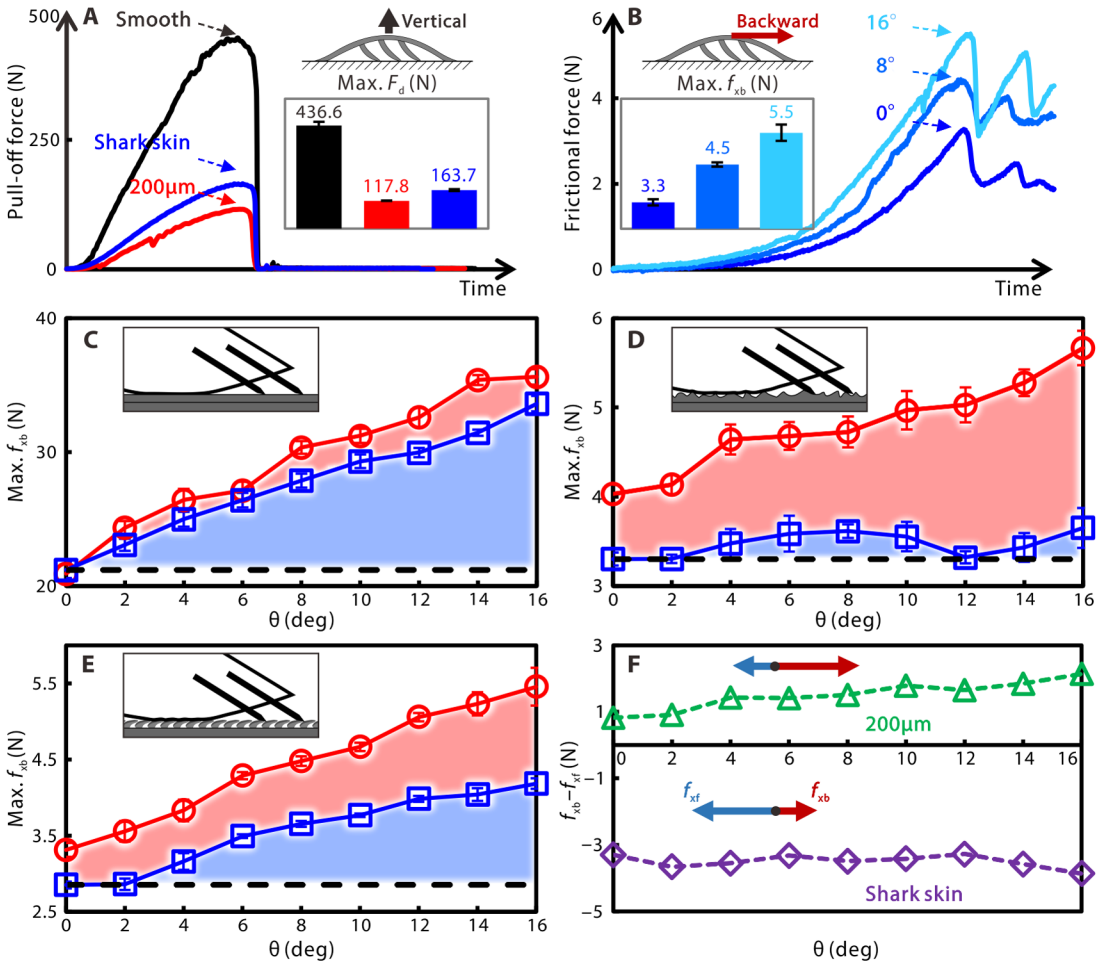


**Fig. 3. Adhesive ability of the biorobotic remora disc prototypes.** (**A**) Pull-off force time series ($F_d$) of the biorobotic disc prototype with artificial spinules on a smooth surface ($R_a$ = 0 μm; black), a real shark skin surface ($R_a$ = 120 μm; blue), and a rough surface ($R_a$ = 200 μm; red). (Inset) Vertically directed pull-off forces (Max. $F_d$) on three surfaces; colors correspond to those in the time history curves. (**B**) Posteriorly directed backward frictional forces ($f_{xb}$) of the disc prototype at different lamella pitch angles θ (0°, 8°, and 16°) on the real shark skin versus time during a representative trial. (Inset) Maximum static frictional forces (Max. $f_{xb}$) at θ = 0°, 8°, and 16° from left to right. (**C** to **E**) Backward frictional forces ($f_{xb}$) of the biorobotic disc prototypes with both lamellae and carbon fiber spinules (red) and lamellae without the artificial spinules (blue) as a function of θ (0° to 16°) on different surfaces. The dashed gray line represents the control prototype without lamellae and spinules. The blue shaded area indicates the contribution of the soft lamella tissue overlay to the frictional force. The red shaded area indicates the contribution of the rigid spinules to the frictional force. (C) Smooth surface. (D) Rough surface ($R_a$ = 200 μm). (E) Real shark skin surface (*I. oxyrinchus*; $R_a \approx$ 120 μm). (**F**) Anisotropic force ($f_{xb} - f_{xf}$) of the disc prototype with carbon fiber spinules versus θ on the rough surface (green) and the shark skin surface (purple).

1.58 N of frictional force with spinules and 0.70 N in the spinule-free control. These results suggest that remoras rely on both the soft tissues of the lamellae and the rigid spinules to enhance the friction force on different surfaces in response to posteriorly directed forces, such as those induced by fluid drag during attachment.

We also found that the lamella pitch motion could significantly enhance the frictional force of the disc prototype. The frictional force with spinules nearly monotonically increased with the lamella pitch angle θ on all three tested surfaces: smooth, rough, and real shark skin (Fig. 3). On the smooth surface, the frictional force of the disc prototype with spinules (red) was almost identical to that without spinules (gray) at θ = 0° but was enhanced 0.7 times at θ = 16° with a frictional stress of $\sigma_{xb}$ = 4.77 kPa ($\sigma_{xb} = f_{xb}/A$, where $A$ represents the disc area) (Fig. 3C). For the disc prototype with spinules, the backward frictional force ($f_{xf}$) increased from 20.93 ± 0.468 N to 35.62 ± 0.579 N when the lamellae were raised from θ = 0° to 16° (ANOVA, df = 8, $F$ = 399.51, $P = 1.963 \times 10^{-7}$). On the rough surface, the frictional force of the prototype with spinules was 16% greater than that of the control at θ = 0° and 55% greater when the lamellae were fully erected to θ = 16° with a frictional stress of $\sigma_{xb}$ = 0.758 kPa (Fig. 3D). The backward frictional force ($f_{xf}$) of the prototype with spinules increased from 4.03 ± 0.102 N to 5.67 ± 0.193 N when the lamellae were raised from 0° to 16° (ANOVA, df = 14, $F$ = 32.42, $P = 7.37 \times 10^{-5}$). On the real shark skin, the frictional force of the prototype with spinules was 16% larger than that of the control at θ = 0° and increased up to 31% at θ = 16°with a frictional stress of $\sigma_{xb}$ = 0.730 kPa (Fig. 3E). The backward frictional force of the prototype with spinules increased from 3.31 ± 0.092 N to 5.46 ± 0.248 N when the lamella angle increased from 0° to 16° (ANOVA, df = 10, $F$ = 76.09, $P = 1.10 \times 10^{-5}$).

The roles of rigid spinules and lamella soft tissue overlay on the frictional anisotropy of the biomimetic remora disc with spinules depend on the properties of the host surface. On the isotropic rough surface ($R_a$ = 200 μm), the forward frictional force ($f_{xf}$) increased from 3.21 ± 0.095 N to 3.53 ± 0.047 N when the lamellae were raised from θ = 0° to 16° (ANOVA, df = 9, $F$ = 10.98, $P$ = 0.0106; fig. S11), and the frictional anisotropy (defined as $f_{xb}/f_{xf}$) of the disc prototype was 1.26 at θ = 0° and 1.61 at θ = 16° (Fig. 3F). On the anisotropic real shark skin surface, the forward frictional force ($f_{xf}$) increased from 6.61 ± 0.107 N to 9.31 ± 0.117 N (ANOVA, df = 9, $F$ = 288.61, $P = 1.42 \times 10^{-7}$; fig. S11), and the frictional anisotropy on the shark skin was 0.5 at θ = 0° and 0.59 at θ = 16° (Fig. 3F). Our results therefore suggest that the lamella pitch motion enhances the forward ($f_{xf}$) and the backward ($f_{xb}$) frictional forces of the prototype on both isotropic and anisotropic rough surfaces. The backward force had a larger magnitude than the forward force on the isotropic surface ($f_{xb}/f_{xf} > 1$), whereas on the anisotropic real shark skin,

Downloaded from http://robotics.sciencemag.org/ by guest on September 23, 2017

the opposite was true ($f_{xb}/f_{xf} < 1$). For remoras, these results suggest that, when they adhere to sharks and other anisotropic surfaces, they are even better at resisting shear force (caused by inertial or external impact) along the anterior direction than the drag force generated in their common attachment direction (water moving from head to tail).

### Underwater attachment and hitchhiking

To explore the potential of our prototypes for integration into autonomous platforms capable of repetitive adhesion, we mounted the biomimetic disc to an underwater remotely operated vehicle (ROV) and demonstrated its performance by executing transitions from free-swimming to stable attachments. The biomimetic disc prototype with artificial spinules was mounted to the underwater vehicle via four springs and four soft fiber-reinforced pneumatic actuators (Fig. 4A). The four springs provided passive alignment between the disc and the overhanging surfaces, and the soft fiber-reinforced actuators could exert a 20-N preload upon pressurization.

The attachment of the disc-containing vehicle was realized in three steps: (i) The vehicle was propelled to an overhanging surface from the bottom of the tank (1.2 m in length, 0.8 m in width, and 1 m in height). (ii) Once the remora disc prototype contacted the surface, the soft actuators were pressurized and generated a preload to push the disc against the surface from below, allowing the artificial spinules to achieve better contact with the local surface asperities. The springs permitted the soft lip of the disc to align with the surface and ensure a dependable suction seal. (iii) All disc lamellae were raised up to increase the capacity for overcoming the external force along the shear directions (Fig. 4B, inset, and movie S6, inset). Last, the vehicle's propellers were switched off to confirm a successful attachment event. To demonstrate system robustness, we repeated the attachment experiments 10 times and observed a 100% success rate, with each attempt taking less than 4 s on average to achieve a stable attachment. For each trial, a significant portion of the time was spent in the swimming phase from the tank bottom to the surfaces located 40 cm above. For demonstration, we also show the underwater vehicle with the remora disc prototype detaching from the substrate and transiting back into the swimming mode (Fig. 4B).

We also varied thrust directions of the three propellers (running at the full speed of 5580 rpm) to create twist (0.45 ± 0.02 N·m), propulsive (6 ± 0.5 N), and pull (4 ± 0.3 N) forces that simulated disturbances encountered by a live remora and complicated flow fields that may be encountered by a disc-equipped underwater vehicle (Fig. 4C). Our underwater vehicle performed robust attachments on a range of natural and artificial surfaces, including noncompliant smooth (Plexiglas), compliant rough [$R_a \approx 200$ μm; fabricated using silicone elastomer (Elastosil M4601, Wacker Chemie AG, München, Germany)], and real shark skin ($R_a \approx 120$ μm; Fig. 4D) surfaces, demonstrating the utility of a self-propelled, hitchhiking underwater vehicle (movie S6).

## DISCUSSION

In this study, we designed and fabricated a biologically inspired, multimaterial prototype modeled upon the disc morphology and lamellar kinematics of the remora sharksucker, *E. naucrates*. The fabrication and actuation of the prototype has several attractive features, and it offers the chance to investigate diverse adhesive disc designs both within and outside of the diversity of forms seen in nature (*2*, *6*). In this way, our prototype provides a platform for investigating the roles of different structural features in remora adhesion while at the same time creating devices that reversibly adhere to a diversity of surfaces underwater.

Using multimaterial 3D printing and laser micromachining to fabricate the disc permits the biologically relevant design of components that varied considerably in Young's modulus from soft (1 MPa for the disc lip and lamella soft tissue overlay) to very rigid (200 GPa for the carbon fiber spinules). Producing spinule-covered, multimaterial lamellae (soft tissue covering the rigid lamella plate) that overlap with undercuts and overhangs is a significant challenge from a traditional design and fabrication perspective (Fig. 1C). This complex morphology is a distinctive characteristic of natural remora discs (*2*) and has been achieved through the use of multimaterial 3D printing and laser micromachining. In addition, the overlapping arrangement of lamellae, which permits more contact with the substrate (Fig. 2H), is a key design feature to enhance friction [Fig. 3C; (*35*)]. Our fabrication process also enables rapid design iteration with little additional cost to change morphological features, including the shape, size, and mechanical stiffness of the components of the remora disc prototype. Such a modular and modifiable system represents great potential as a tool to examine the adhesive contributions of the diverse disc morphologies and lamellar kinematic patterns represented by the eight species within the family Echeneidae that adhere to a wide range of different hosts (*2*, *6*).

With our disc prototype, we were able to mimic the raising and folding movements of the lamellae by controlling lamella pitch with soft pneumatic actuators. Although the pitch amplitudes of the soft-actuated biomimetic disc prototype exceeded the pitch range of the biological lamellae, they can be controlled precisely and, thus, be constrained within the range of biologically relevant values (Fig. 2E).

Because the mechanical properties of the remora disc soft tissues (fleshy disc lip and soft lamella overlay) are similar to those of fish skin (Young's modulus of 0.5 MPa) (2, *36*), we were unable to precisely match the mechanical properties of the disc prototype (e.g., the soft tissue overlay that surrounds the overhanging rigid lamella plate and the soft tissue that connects the disc lip and the lamellae) to their biological analogs using current multimaterial 3D printing approaches. However, improvements in 3D printing technology in the future may allow for the reproduction of more flexible materials in the range of biological soft tissues for the production of more lifelike prototypes. In addition, we demonstrated disc detachment with a simplified engineering approach (by pumping water into the disc to eliminate the chamber pressure differential) to achieve a remora-like hitchhiking behavior. However, understanding the detachment behavior of remoras would require additional comprehensive studies that include morphological and kinematic measurements of live remoras. The ability to incorporate the detachment capability into the disc prototype with a new biologically inspired mechanism in the future would complement our current disc design.

Our biomimetic disc prototype demonstrated the ability to attach to a variety of surfaces, including smooth (epoxy resin), rough (epoxy resin), compliant rough (silicone elastomer), and real shark skin ($R_a$ = 120 μm), and enabled an underwater ROV with the ability to hitchhike onto these surfaces. Through the fabrication process and the experiments conducted on the disc prototype, we investigated the function of different morphological disc features on adhesion.

First, the soft disc lip functions as a suction seal that contributes directly to produce a considerable pull-off force up to 438 N (approximately 340 times the weight of the disc prototype). The remora disc prototype showed similar pull-off stress (58.7 kPa) on the smooth

Downloaded from http://robotics.sciencemag.org/ by guest on September 23, 2017

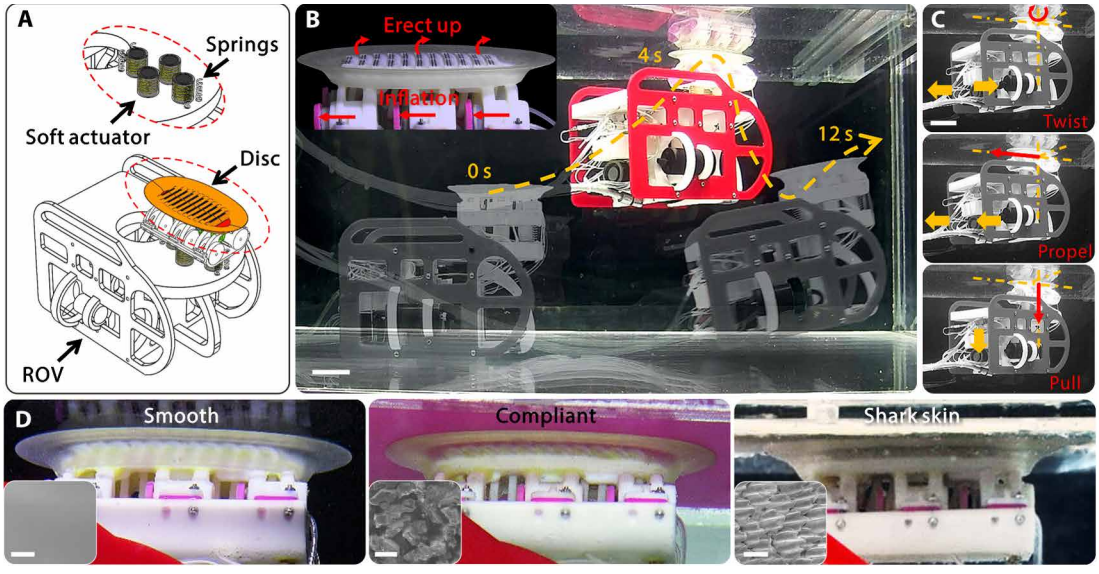


**Fig. 4. Attachment of an underwater vehicle using the biorobotic remora disc.** (**A**) The remora disc prototype is connected to the ROV via four springs with low stiffness and four soft silicone pneumatic elastomer actuators. The ROV contains three propellers with a motor power rating of 300 W for each. The mass of the robot is 1.46 kg. (**B**) Frames of attachment of the robot from movie S6 at various time instants. The ROV with the remora disc prototype performs a successful transition from a swimming mode (propelled by rotors) to the attachment mode (4 s) on a smooth glass surface. For demonstration purposes, we also show the remora disc ROV detaching from the surface and transitioning back into the swimming mode (12 s). For simplification, we used a syringe to pump water into the chamber for balancing the pressure difference between the interior and exterior of the disc chamber for detachment. Scale bar, 50 mm. (**C**) Remora disc ROV after successful attachment to the surface and attachment against propelling, twisting, and pulling. Scale bar, 50 mm. (**D**) As with the isolated disc prototype studies, the ROV can successfully attach to various surfaces, including smooth (Plexiglas; left), compliant rough (silicone elastomer; middle), and real shark skin (right). Scale bars, 200 μm.

surface compared with commercial suction cups (50 to 80 kPa). However, the remora disc prototype produced substantially greater pull-off stress (15.8 to 21.9 kPa on surface of roughness $R_a$ = 200 μm) relative to commercially available suction cups on rough surfaces [which fail to stick to surfaces with $R_a$ > 21.8 μm; (*14*)]. Second, by raising the spinule-covered composite lamellae in the disc interior, similar to its biological counterparts, the frictional force can be significantly enhanced on both smooth and rough surfaces, up to 1.7 and 1.4 times, respectively. Third, our prototype experimental data demonstrated that the rigid spinules and the soft tissue overlaying the lamellae work in concert and contribute differentially to enhancing frictional forces during remora attachment on surfaces with different roughness. For example, on the smooth surface, we observed that prototypes with and without spinules generate similar amounts of posteriorly directed frictional forces. In contrast, for adhesion to the rough surface ($R_a \approx$ 200 μm), spinules contributed more to the frictional force than the soft tissue overlay made of soft material (Fig. 3D). On the real shark skin, a common natural host surface for *E. naucrates* [$R_a \approx$ 120 μm; (*30*)], both the lamella soft tissue overlay and the rigid spinules play essential roles (Fig. 3E, inset). A friction theoretical model was developed to evaluate the spinule contribution to the shear force (*31*), suggesting that spinules are primarily responsible for friction enhancement on rough surfaces, which agrees with our current finding. To summarize, the frictional force on the disc prototype can be significantly increased because of the combination of the rigid spinules and the lamella soft tissue overlay in response to different surface roughness. On rougher surfaces, the disc prototype always produced higher frictional forces with spinules than without spinules.

We consider hitchhiking as an effective strategy for reducing energy expenditure during transport or movement of small underwater robots. Like robotic propulsion, live fishes (including remoras) require body muscular power to generate thrust during swimming (*37*–*39*), whereas nearly zero muscular power is needed when attaching to a substrate (*2*, *40*). The shape of the remora is similar to that of a streamlined body, with a low drag coefficient well suited for hitchhiking (*39*). For example, a 35-cm remora attached to a 2 m/s swimming (*3*) bottlenose dolphin (*Tursiops truncatus*) with a relatively smooth surface ($R_a$ < 20 μm) would incur only 0.27 N of drag (*39*). Our disc prototype can produce a frictional force on a smooth surface, which is up to 132 times the drag experienced by a remora attached to a host swimming at 2 m/s (*39*). Attached to a real shark skin substrate, our disc prototype produced frictional forces up to 34 times the estimated drag force of 0.16 N for a 35-cm remora attached to a shortfin mako (*I. oxyrinchus*), a host with rough skin ($R_a \approx$ 120 μm), swimming at an average cruising speed of 1.5 m/s.

This adhesive technology also offers possible utility for gripping applications underwater [e.g., in a dynamic tanker docking engineering system as described in (*16*)] or in air (movie S7), which requires adhesive forces in both the normal and shear directions. As demonstrated here, the attachment dynamics of our remora disc prototype thus permits high-performance underwater adhesion. Coupled with a platform of streamlined shape, such a system could markedly reduce transport and movement costs and increase mission durations for autonomous underwater vehicles.

## MATERIALS AND METHODS

### Morphology and kinematics of the biological remora disc

To reveal the structural details of the remora skeletal system, we scanned, segmented, and reconstructed a preserved remora (*E. naucrates*) adhesive disc using microcomputed tomography (microCT) (movie S1). Using an environmental scanning electron microscope (ESEM), we also measured the geometries of more than 30 spinule samples from remora discs. More details on the morphological measurements can be found in section S2. All the live remoras used in this study were handled in accordance with the Regulations for the Administration of Affairs Concerning Experimental Animals issued by the Institutional

Downloaded from http://robotics.sciencemag.org/ by guest on September 23, 2017

Animal Care and Use Committee of Beijing. To characterize the lamella kinematics, we quantified their movement using high-speed videography (Fig. 2A and fig. S1). Because the lamella movement was not visible from a side-view camera, we extracted the movement data ($x$ axis) of marker points to analyze the lamellar kinematics from dorsal-view images (Fig. 2, A and B). More detailed descriptions on lamella locomotion analysis are found in section S1.

### Design and fabrication of the remora disc

On the basis of the previously described morphological and kinematic features, we developed a computer-aided design (CAD) model for the fabrication of the disc prototype (Fig. 1C). The primary components were designed by mimicking the dominant geometries of the natural lamella plate and disc base of microCT-scanned remora specimens. In lateral view, the spinule tips overlap with the base of the adjacent posterior lamellae (the right inset image in Fig. 1C). The biomimetic disc lip surrounds the disc base as an anchoring structure to enhance the surface area of the bonding interface (the left inset image in Fig. 1C). In addition, a soft tissue connects the lateral aspects of the lamellae to the disc lip (fig. S5C). More detailed descriptions on the design and fabrication of the disc main body, the carbon fiber spinules, and the soft actuators that erect or fold the lamellae are provided in section S3.

### Forces and pressure measurements of the prototypes

We investigated the effects of pitchable lamellae and rigid spinules on the adhesive performance of the disc while in contact with surfaces of different roughness in water. We tested each disc prototype on two nonbiological rigid surfaces, one smooth and one rough surface [$R_a \approx 200$ μm; by both molding and casting with epoxy resin material (EpoxAcast 650, Smooth-On Inc., PA); fabrication details are provided in section S5], and on real shark skin ($R_a \approx 120$ μm; preparation details are provided in section S5) (fig. S7). To measure the pull-off force ($F_d$) and the frictional force ($f_d$), we tested the submerged prototype with a multiple-axis force transducer mounted to a robotic arm (fig. S6). To evaluate the differential contribution of lamella soft tissue overlay and rigid spinules in the generation of frictional force on surfaces of different roughness, we fabricated two biorobotic remora disc prototypes: one with the lamella soft tissue only (i.e., without spinules; fig. S5A) and another with biomimetic spinules (fig. S5B). Using these disc prototypes, we further determined the pull-off force and static frictional force as a function of the lamella pitch angle θ (0° to 16°). More detailed descriptions on forces and pressure measurements of the prototypes are provided in section S5.

## SUPPLEMENTARY MATERIALS

robotics.sciencemag.org/cgi/content/full/2/10/eaan8072/DC1

Text

Fig. S1. Experimental setup for remora locomotion observation during attachment and schematic diagrams of lamella kinematic analysis.

Fig. S2. Design details of the lamella plates and the artificial spinules.

Fig. S3. Fabrication procedures of the whole remora disc prototype.

Fig. S4. Design and fabrication of the soft actuators.

Fig. S5. Two prototypes (disc with lamellae only without spinules and disc with lamellae and with spinules) tested in this study.

Fig. S6. Experimental setup of forces and pressure measurements.

Fig. S7. ESEM images of three substrates and setup for the side-view contact visualization.

Fig. S8. Dimensionless amplitude of the lamellae's marker point $u$ versus time for the folding down motions of a live remora and the biomimetic remora disc.

Fig. S9. The fully ambient pressure differential of the prototype chamber versus the lamella pitch angle (θ) when the disc was attached to a smooth substrate.

Fig. S10. Pressure of the chamber during a complete pull-off process.

Fig. S11. Forward frictional forces on the (A) shark skin surface and (B) rough surface ($R_a = 200$ μm).

Table S1. Morphological parameters of three individual remoras and their adhesive discs.

Table S2. Physical parameters of the disc prototype and the lamellae.

Table S3. Length of the artificial spinule plates of the disc prototype.

Table S4. Geometry of a single laser-cut biomimetic spinule and the spinule plate.

Table S5. Stiffness of the components in the biomimetic prototype.

Movie S1. Demonstration of a remora's adhesive disc in the microCT data.

Movie S2. Remora lamella motion recorded by a high-speed camera (erect up and fold down).

Movie S3. Animation of lamella pitching mechanism.

Movie S4. Lamella motion of the biomimetic adhesive disc.

Movie S5. Lamella motion comparison between the biological and biomimetic adhesive disc (erect up and fold down, on the transparent glass surface).

Movie S6. Demonstration of the underwater attachment of the biorobotic remora disc via an underwater robotic system.

Movie S7. Demonstration of the biorobotic remora disc gripping a variety of items in air.

References (*41*–*43*)

## REFERENCES AND NOTES


1. A. Günther, XLII.—On the history of *Echeneis*. *J. Nat. Hist.* **5**, 386–402 (1860).
2. B. A. Fulcher, P. J. Motta, Suction disk performance of *Echeneid* fishes. *Can. J. Zool.* **84**, 42–50 (2006).
3. D. Weihs, F. E. Fish, A. J. Nicastro, Mechanics of remora removal by dolphin spinning. *Mar. Mamm. Sci.* **23**, 707–714 (2007).
4. R. F. Cressey, E. A. Lachner, The parasitic copepod diet and life history of diskfishes (*Echeneidae*). *Copeia* **2**, 310–318 (1970).
5. J. F. Steffensen, J. P. Lomholt, Energetic cost of active branchial ventilation in the sharksucker, *Echeneis naucrates*. *J. Exp. Biol.* **103**, 185–192 (1983).
6. R. Britz, G. D. Johnson, Ontogeny and homology of the skeletal elements that form the sucking disc of remoras (*Teleostei*, *Echeneoidei*, *Echeneidae*). *J. Morphol.* **273**, 1353–1366 (2012).
7. M. Friedman, Z. Johanson, R. C. Harrington, T. J. Near, M. R. Graham, An early fossil remora (*Echeneoidea*) reveals the evolutionary assembly of the adhesion disc. *Proc. R. Soc. B* **280**, 20131200 (2013).
8. K. Autumn, Y. A. Liang, S. T. Hsieh, W. Zesch, W. P. Chan, T. W. Kenny, R. Fearing, R. J. Full, Adhesive force of a single gecko foot-hair. *Nature* **405**, 681–685 (2000).
9. D.-M. Drotlef, L. Stepien, M. Kappl, W. J. P. Barnes, H.-J. Butt, A. del Campo, Insights into the adhesive mechanisms of tree frogs using artificial mimics. *Adv. Funct. Mater.* **23**, 1137–1146 (2013).
10. W. Federle, W. J. P. Barnes, W. Baumgartner, P. Drechsler, J. M. Smith, Wet but not slippery: Boundary friction in tree frog adhesive toe pads. *J. R. Soc. Interface* **3**, 689–697 (2006).
11. J. H. Lai, J. C. del Alamo, J. Rodríguez-Rodríguez, J. C. Lasheras, The mechanics of the adhesive locomotion of terrestrial gastropods. *J. Exp. Biol.* **213**, 3920–3933 (2010).
12. D. Dodou, P. Breedveld, J. C. F. de Winter, J. Dankelman, J. L. van Leeuwen, Mechanisms of temporary adhesion in benthic animals. *Biol. Rev.* **86**, 15–32 (2011).
13. D. Labonte, W. Federle, Scaling and biomechanics of surface attachment in climbing animals. *Philos. Trans. R. Soc. Lond. B Biol. Sci.* **370**, 20140027 (2015).
14. D. K. Wainwright, T. Kleinteich, A. Kleinteich, S. N. Gorb, A. P. Summers, Stick tight: Suction adhesion on irregular surfaces in the northern clingfish. *Biol. Lett.* **9**, 20130234 (2013).
15. P. Ditsche, D. K. Wainwright, A. P. Summers, Attachment to challenging substrates—Fouling, roughness and limits of adhesion in the northern clingfish (*Gobiesox maeandricus*). *J. Exp. Biol.* **217**, 2548–2554 (2014).
16. T. I. Wolff, "The design and fabrication of a biomimetic lifting aid," thesis, University of Twente, Enschede, Overijssel (2017).
17. C. Li, T. Zhang, D. I. Goldman, A terradynamics of legged locomotion on granular media. *Science* **339**, 1408–1412 (2013).
18. E. Kizilkan, J. Strueben, A. Staubitz, S. N. Gorb, Bioinspired photocontrollable microstructured transport device. *Sci. Robot.* **2**, eaak9454 (2017).
19. U. Çulha, F. Iida, Enhancement of finger motion range with compliant anthropomorphic joint design. *Bioinspir. Biomim.* **11**, 026001 (2016).
20. J.-S. Koh, E. Yang, G.-P. Jung, S.-P. Jung, J. H. Son, S.-I. Lee, P. G. Jablonski, R. J. Wood, H.-Y. Kim, K.-J. Cho, Jumping on water: Surface tension–dominated jumping of water striders and robotic insects. *Science* **349**, 517–521 (2015).
21. M. Wehner, R. L. Truby, D. J. Fitzgerald, B. Mosadegh, G. M. Whitesides, J. A. Lewis, R. J. Wood, An integrated design and fabrication strategy for entirely soft, autonomous robots. *Nature* **536**, 451–455 (2016).
22. L. Wen, J. C. Weaver, G. V. Lauder, Biomimetic shark skin: Design, fabrication and hydrodynamic function. *J. Exp. Biol.* **217**, 1656–1666 (2014).


Downloaded from http://robotics.sciencemag.org/ by guest on September 23, 2017

23. M. M. Porter, D. Adriaens, R. L. Hatton, M. A. Meyers, J. McKittrick, Why the seahorse tail is square. *Science* **349**, aaa6683 (2015).
24. H.-T. Lin, G. G. Leisk, B. Trimmer, GoQBot: A caterpillar-inspired soft-bodied rolling robot. *Bioinspir. Biomim.* **6**, 026007 (2011).
25. S. A. Morin, R. F. Shepherd, S. W. Kwok, A. A. Stokes, A. Nemiroski, G. M. Whitesides, Camouflage and display for soft machines. *Science* **337**, 828–832 (2012).
26. D. Rus, M. T. Tolley, Design, fabrication and control of soft robots. *Nature* **521**, 467–475 (2015).
27. N. W. Bartlett, M. T. Tolley, J. T. Overvelde, J. C. Weaver, B. Mosadegh, K. Bertoldi, G. M. Whitesides, R. J. Wood, A 3D-printed, functionally graded soft robot powered by combustion. *Science* **349**, 161–165 (2015).
28. S.-J. Park, M. Gazzola, K. S. Park, S. Park, V. Di Santo, E. L. Blevins, J. U. Lind, P. H. Campbell, S. Dauth, A. K. Capulli, F. S. Pasqualini, S. Ahn, A. Cho, H. Yuan, B. M. Maoz, R. Vijaykumar, J.-W. Choi, K. Deisseroth, G. V. Lauder, L. Mahadevan, K. K. Parker, Phototactic guidance of a tissue-engineered soft-robotic ray. *Science* **353**, 158–162 (2016).
29. M. A. Graule, P. Chirarattananon, S. B. Fuller, N. T. Jafferis, K. Y. Ma, M. Spenko, R. Kornbluh, R. J. Wood, Perching and takeoff of a robotic insect on overhangs using switchable electrostatic adhesion. *Science* **352**, 978–982 (2016).
30. B. O'Toole, Phylogeny of the species of the superfamily Echeneoidea (Perciformes: Carangoidei: Echeneidae, Rachycentridae, and Coryphaenidae), with an interpretation of echeneid hitchhiking behaviour. *Can. J. Zool.* **80**, 596–623 (2002).
31. M. Beckert, B. E. Flammang, J. H. Nadler, Remora fish suction pad attachment is enhanced by spinule friction. *J. Exp. Biol.* **218**, 3551–3558 (2015).
32. P. B. Moyle, J. J. Cech, *Fishes: An Introduction to Ichthyology* (Prentice Hall, 1996).
33. B. C. Jayne, A. F. Lozada, G. V. Lauder, Function of the dorsal fin in bluegill sunfish: Motor patterns during four distinct locomotor behaviors. *J. Morphol.* **228**, 307–326 (1996).
34. V. Pavlov, B. Rosental, N. F. Hansen, J. M. Beers, G. Parish, I. Rowbotham, B. A. Block, Hydraulic control of tuna fins: A role for the lymphatic system in vertebrate locomotion. *Science* **357**, 310–314 (2017).
35. B. Lorenz, B. A. Krick, N. Rodriguez, W. G. Sawyer, P. Mangiagalli, B. N. J. Persson, Static or breakloose friction for lubricated contacts: The role of surface roughness and dewetting. *J. Phys. Condens. Matter* **25**, 1–22 (2013).
36. A. P. Summers, J. H. Long Jr., Skin and bones, sinew and gristle: The mechanical behavior of fish skeletal tissues. *Fish Physiol.* **23**, 141–177 (2005).
37. L. C. Rome, D. Swank, D. Corda, How fish power swimming. *Science* **261**, 340–343 (1993).
38. J. C. Liao, D. N. Beal, G. V. Lauder, M. S. Triantafyllou, Fish exploiting vortices decrease muscle activity. *Science* **302**, 1566–1569 (2003).
39. M. Beckert, B. E. Flammang, E. J. Anderson, J. H. Nadler, Theoretical and computational fluid dynamics of an attached remora (*Echeneis naucrates*). *Zoology* **119**, 430–438 (2016).
40. S. L. Hora, The adhesive apparatus of the "sucking fish". *Nature* **115**, 48 (1925).
41. T. L. Hedrick, Software techniques for two- and three-dimensional kinematic measurements of biological and biomimetic systems. *Bioinspir. Biomim.* **3**, 1–6 (2008).
42. M. Scherge, S. Gorb, S. N. Gorb, *Biological Micro- and Nanotribology* (Springer Science & Business Media, 2001).
43. J. N. Israelachvili, *Intermolecular and Surface Forces: Revised Third Edition* (Academic Press, 2011).


**Acknowledgments:** We thank X. Ling and L. Bao for their contribution to this work and G. Lauder for providing comments to this paper. **Funding:** This work was supported by the National Science Foundation of China support projects (grant nos. 61403012 and 61633004 to L.W.), the Wyss Institute for Biologically Inspired Engineering, NSF Postdoctoral Fellowship in Biology award no. 1103761 (to C.P.K.), and NSF Graduate Research Fellowship 2014162421 (to D.K.W.). **Author contributions:** C.P.K., R.J.W., and L.W. conceived the project. Y.W., Y.C., and L.W. designed and fabricated the biomimetic remora disc. Y.W., C.P.K., D.K.W., H.L., J.C.W., and L.W. characterized the morphology of the biological remora disc. X.Y., Y.W., Z.L., C.P.K., and L.W. conducted the kinematics of the remora disc. Y.W., X.Y., Y.C., D.K.W., and L.W. conducted the adhesive measurements and analyzed the data. Z.G., Z.L., and L.W. conducted underwater robot attachment experiments. L.W. and X.Y. prepared the manuscript, and all authors provided feedback during subsequent revisions. **Competing interests:** Patents have been submitted to the Chinese Patent Office, describing the remora-inspired underwater adhesive disc. Y.W., Y.C., and L.W. are authors of patent application 201710309248X. **Data and materials availability:** Please contact L.W. for data and other materials.

Submitted 22 May 2017
Accepted 28 August 2017
Published 20 September 2017
10.1126/scirobotics.aan8072

**Citation:** Y. Wang, X. Yang, Y. Chen, D. K. Wainwright, C. P. Kenaley, Z. Gong, Z. Liu, H. Liu, J. Guan, T. Wang, J. C. Weaver, R. J. Wood, L. Wen, A biorobotic adhesive disc for underwater hitchhiking inspired by the remora suckerfish. *Sci. Robot.* **2**, eaan8072 (2017).

Downloaded from http://robotics.sciencemag.org/ by guest on September 23, 2017

Science Robotics

# A biorobotic adhesive disc for underwater hitchhiking inspired by the remora suckerfish

Yueping Wang, Xingbang Yang, Yufeng Chen, Dylan K. Wainwright, Christopher P. Kenaley, Zheyuan Gong, Zemin Liu, Huan Liu, Juan Guan, Tianmiao Wang, James C. Weaver, Robert J. Wood and Li Wen

*Sci. Robotics* **2**, eaan8072.
DOI: 10.1126/scirobotics.aan8072

**ARTICLE TOOLS** http://robotics.sciencemag.org/content/2/10/eaan8072

**SUPPLEMENTARY MATERIALS** http://robotics.sciencemag.org/content/suppl/2017/09/18/2.10.eaan8072.DC1

**REFERENCES** This article cites 39 articles, 19 of which you can access for free
http://robotics.sciencemag.org/content/2/10/eaan8072#BIBL

**PERMISSIONS** http://www.sciencemag.org/help/reprints-and-permissions

Use of this article is subject to the Terms of Service

*Science Robotics* (ISSN 2470-9476) is published by the American Association for the Advancement of Science, 1200 New York Avenue NW, Washington, DC 20005. 2017 © The Authors, some rights reserved; exclusive licensee American Association for the Advancement of Science. No claim to original U.S. Government Works. The title *Science Robotics* is a registered trademark of AAAS.

Downloaded from http://robotics.sciencemag.org/ by guest on September 23, 2017